

A multi-resolution analysis based finite element model updating method for damage identification

Xin Zhang^{*1}, Danying Gao¹, Yang Liu¹ and Xiuli Du²

¹Zhengzhou University, Zhengzhou, P.R. China

²Beijing University of Technology, Beijing, P.R. China

(Received April 24, 2013, Revised April 27, 2014, Accepted August 1, 2014)

Abstract. A novel finite element (FE) model updating method based on multi-resolution analysis (MRA) is proposed. The true stiffness of the FE model is considered as the superposition of two pieces of stiffness information of different resolutions: the pre-defined stiffness information and updating stiffness information. While the resolution of former is solely decided by the meshing density of the FE model, the resolution of latter is decided by the limited information obtained from the experiment. The latter resolution is considerably lower than the former. Second generation wavelet is adopted to describe the updating stiffness information in the framework of MRA. This updating stiffness in MRA is realized at low level of resolution, therefore, needs less number of updating parameters. The efficiency of the optimization process is thus enhanced. The proposed method is suitable for the identification of multiple irregular cracks and performs well in capturing the global features of the structural damage. After the global features are identified, a refinement process proposed in the paper can be carried out to improve the performance of the MRA of the updating information. The effectiveness of the method is verified by numerical simulations of a box girder and the experiment of a three-span continuous pre-stressed concrete bridge. It is shown that the proposed method corresponds well to the global features of the structural damage and is stable against the perturbation of modal parameters and small variations of the damage.

Keywords: model updating; multi-resolution analysis; damage identification and second generation wavelet

1. Introduction

The finite element (FE) model updating technique is to calibrate the numerical models against the real structures (Mottershead *et al.* 2011). It can also be used to identify structural damages (Yu and Chung 2012, Yun *et al.* 2009).

The FE model is updated by minimizing the penalty function reflecting the differences between the measured and calculated system properties. Many forms of penalty functions have been developed in the literatures. These penalty functions may be based on the residues of frequencies and mode shapes (Brownjohn *et al.* 2001), modal flexibility (Jaishi and Ren 2006), transfer functions (Esfandiari *et al.* 2010, Imregun *et al.* 1995) or frequencies and strain energies (Jaishi and Ren 2007), etc. The optimization method used to minimize the penalty function include,

*Corresponding author, Professor, E-mail: zhangxin@zzu.edu.cn

among others, sensitivity-based methods (Mottershead *et al.* 2011, Bakir *et al.* 2007), genetic algorithm (GA) (Levin and Lieven 1998) and evolutionary algorithm (EA) (Kyprianou *et al.* 2001).

An inherent weakness of the updating process is the indeterminacy: the FE model of a real structure is usually complex requiring a large number of parameters to be updated while the information that can be extracted from the experimental data is, unfortunately, very limited. In this case, the updating process will be both inefficient and unreliable.

Therefore, in order to improve the efficiency of the updating process, not only do we need improved optimization methods (Zapico-Valle *et al.* 2010), but also an educated guess to limit the number of updating parameters. The response surface method (Ren and Chen 2010) is an effort of this type to calibrate a limited number of structural parameters according to measured responses. The updating process is more stable in this case compared with traditional updating processes. Damage function method (Teughels *et al.* 2002, Fang 2008) and the automatic parameter selection method (Kim and Park 2008) are with the similar objective to limit the number of parameters involved in the updating process. The multistage updating strategy (Perera and Ruiz 2008, Weng *et al.* 2011, Law *et al.* 2001, Titurus *et al.* 2003) proposes the idea of two-stage damage identification. These methods locate the damage roughly at the global level in the first step and perform a finer identification to identify the damages at local level in the second step. These methods may also reduce the number of updating parameters.

Despite all these efforts, problems still exist. For instance, concrete structures, the most important type of structures in civil engineering, may have very complex damage patterns, such as multiple irregular cracks or multiple groups of irregular cracks. This issue poses a critical challenge to the selection of damage parameters if the aforementioned methods are adopted because none of the information about the position, number or the shape of cracks is known before hand.

In the paper, we try to solve this problem. A novel method based on multi-resolution analysis (MRA) is proposed to capture the global feature of the damage automatically.

2. The multi-resolution strategy for FE model updating

Fig. 1 shows the example of beams. Fig. 1(a) shows an un-cracked beam, Fig. 1(b) shows a beam with only one crack and fig1.c shows a beam with multiple irregular cracks. The stiffness of each beam is also shown in the right column of the figure. The reductions of the stiffness due to the cracks are indicated in figures by the “real curve” in solid lines.

The ideal objective of the model updating is to update the stiffness of the beam in Fig. 1 to find the best-fit of the “real curves”. In doing so, we need a relatively finely meshed FE model so that the variations in the stiffness may be reflected clearly. Because the number, positions and the sizes of these cracks are not known before hand, the researchers may not be able to tell which beam, 1.b or 1.c, need to be modeled with finer elements. As a result, two beams may be modeled at the same level of precision or resolution. (In this paper, a FE model with a finer mesh is termed as a model of higher resolution.)

During the updating process, it is usually supposed that:

- 1) The experimental modal parameters are retrieved by modal testing methods;
- 2) Measurements of acceleration time history are made at a limited number of positions,
- 3) The identified modes are displacement modes;
- 4) The values of the mode shapes are known only at the measurement points up to the

accuracy of experiments, i.e., the mode shapes have a limited resolution;

- 5) The measured frequencies are of limited accuracy also;
- 6) Only a small number of structural modes and corresponding frequencies are available for FE model updating.

We face a dilemma here. The ideal objective of model updating needs the FE model to be meshed as finely as possible, while the limited experimental information only tends to support the updating of very few parameters. Under the circumstances, it would be more practical to find the approximated curves of stiffness shown in Fig. 1 instead of the real curves. If the approximated curves are well defined, the modal parameters from the approximated curves will be close to those modal parameters from the real curves.

The approximated curve corresponds to the global feature of the damage. The approximated curve is a low resolution version of the “real curve”. The former has smaller variations than the latter. Therefore, it needs less data points to represent.

A parallel situation is the wavelet decomposition (Mallat 2009) of signals to find the trend line (approximated curve) by removing the higher frequency components from a data series. However, a direct wavelet decomposition of the “real curve” is not suitable here, as we need to constrain the decomposition with the similarity of modal parameters between the experimental model and the updated FE model. The “approximated curve” in this case is usually not the replica of the trend line of wavelet decomposition.

3. FE model updating based on MRA

The true stiffness of a structure, $K(x)$, i.e., the real curve in fig.1.b&c, can be seen as the summation of two curves

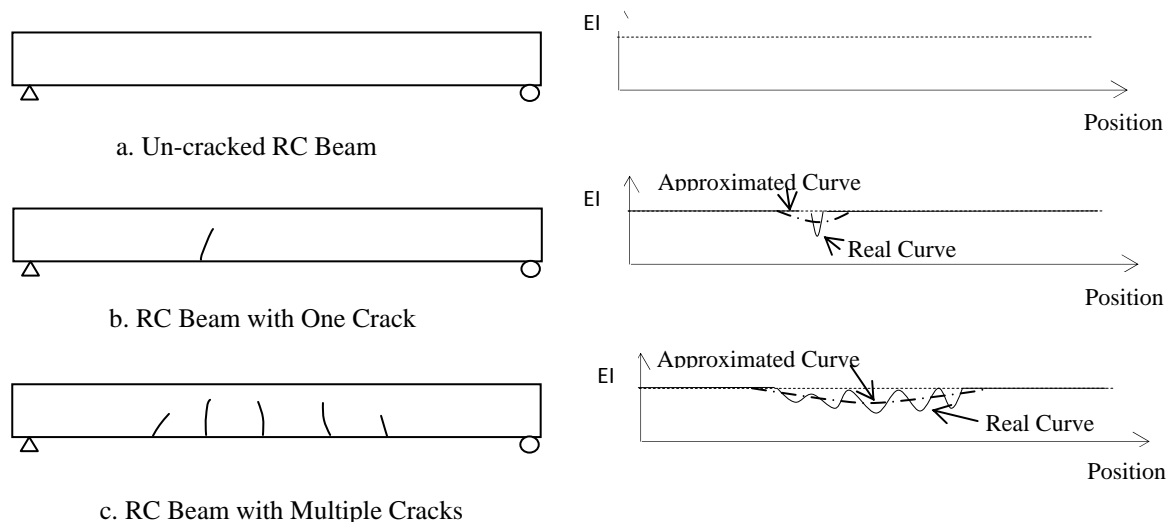


Fig. 1 Example Beam

$$\mathbf{K}(x) = K(x) + \boldsymbol{\kappa}(x) \quad (1)$$

where $K(x)$ is the pre-defined stiffness at position x , and $\boldsymbol{\kappa}(x)$ is the updating function of stiffness. While the resolution of $K(x)$ is determined by the meshing density of the finite element model, the resolution of $\boldsymbol{\kappa}(x)$ corresponds to the quantity of information that can be extracted from the experiment. Usually, the FE model needs to be meshed as finely as necessary to produce accurate computational results, giving rise to a relatively high resolution to the pre-defined stiffness function, $K(x)$. The experiments, however, can only provide very limited modal information to be used. As a result, the updating stiffness function, $\boldsymbol{\kappa}(x)$, has a poorer resolution.

If j is the pre-determined level of resolution, the approximation of space V of $\boldsymbol{\kappa}(x)$ at level j and $j+1$ are V_j and V_{j+1} , respectively. The difference space is $W_j = V_{j+1} / V_j$.

V_j is spanned by the scaling function $\phi_{j,k}(x-k)$

$$V_j = \text{span}\{\phi_{j,k}(x) \mid \phi_{j,k}(x) = 2^{j/2} \phi(2^j x - k), k \in \mathbb{Z}\} \quad (2)$$

the difference space, $W_j = V_{j+1} / V_j$ is spanned by the wavelet function, $\psi_{j,k}(x-k)$

$$W_j = \text{span}\{\psi_{j,k}(x) \mid \psi_{j,k}(x) = 2^{j/2} \psi(2^j x - k), k \in \mathbb{Z}\} \quad (3)$$

where k is the sampling position.

A low resolution form of $\boldsymbol{\kappa}(x)$ at approximation level j may be achieved

$$\boldsymbol{\kappa}^j(x) = \sum_{k \in \mathbb{Z}} c_k^j \phi_{j,k}(x) \quad (4)$$

And at approximation level $j+1$

$$\boldsymbol{\kappa}^{j+1}(x) = \sum_{k \in \mathbb{Z}} c_k^j \phi_{j,k}(x) + \sum_{k \in \mathbb{Z}} d_k^j \psi_{j,k}(x) \quad (5)$$

The larger the value of j , the more accurately the stiffness function is represented, however, at the cost of using more detail and approximation coefficients d_k^j and c_k^j , and vice versa. In the wavelet analysis

$$c_k^j = \langle \boldsymbol{\kappa}(x), \tilde{\phi}_{j,k}(x) \rangle, d_k^j = \langle \boldsymbol{\kappa}(x), \tilde{\psi}_{j,k}(x) \rangle \quad (6)$$

where $\tilde{\phi}_{j,k}(x)$ is the dual of $\phi_{j,k}(x)$ and $\tilde{\psi}_{j,k}(x)$ is the dual of $\psi_{j,k}(x)$ (Mallat 2009). However, (6) is not true in our case because the approximated stiffness function has to satisfy the eigen-function of structural dynamics. Therefore, the values of c_k^j and d_k^j have to be found by model updating process.

Let $\boldsymbol{\alpha} = \{c_k^j, d_k^j\}, k = 1, 2, 3, \dots$ be the state vector. The modal parameters of the FE model are $(\lambda_i, \varphi_i), i = 1, 2, \dots$, where λ_i is the i^{th} frequency and φ_i is the i^{th} mode shape. The experimental

modal parameters are $(\bar{\lambda}_i, \bar{\varphi}_i), i = 1, 2, \dots$. The error index vector is defined as

$$\{r(\alpha)\} = \begin{Bmatrix} r_f(\alpha) \\ r_s(\alpha) \end{Bmatrix} = W \begin{Bmatrix} \bar{\lambda}_1 - \lambda_1 \\ \vdots \\ \bar{\lambda}_m - \lambda_m \\ 1 - MAC_1 \\ \vdots \\ 1 - MAC_m \end{Bmatrix} \quad (7)$$

where weights are introduced to balance the relative importance of different modal parameters

$$W = \text{diag}(1/\bar{\lambda}_1, \dots, 1/\bar{\lambda}_m, n_1, \dots, n_m) \quad (8)$$

The Modal Amplitude Coherence for the i^{th} mode is defined as

$$MAC_i = |\bar{\varphi}_i \varphi_i^*| / (|\bar{\varphi}_i \bar{\varphi}_i^*| |\varphi_i \varphi_i^*|)^{0.5} \quad (9)$$

In (8), $n_i = 1$ for well identified mode shapes; $n_i < 1$ for poorly identified mode shapes. Mode shapes are needed in the updating process to make sure the corresponding frequency belongs to the same mode. However, in practice, some of the mode shapes may be identified poorly. For practical purpose, we use smaller weights for these poorly identified mode shapes so that the modal testing error will not affect the updating process too much.

The objective of the model updating process is to minimize the norm of the vector $\{r(\alpha)\}$

$$\min \|\{r(\alpha)\}\|, \alpha = \{c_i, d_i\}, i = 1, 2, \dots \quad (10)$$

If the approximation coefficients at level j are to be found, we use the state vector, $\alpha = \{c_k^j\}, k = 1, 2, 3, \dots$, as the updating parameters. To go to the next finer level, we have two options: adding detail coefficients to the state vector $\alpha = \{c_k^j, d_k^j\}, k = 1, 2, 3, \dots$, or use $\alpha = \{c_k^{j+1}\}, k = 1, 2, 3, \dots$.

If the first option is adopted, the optimization at the finer level of resolution can be performed by supplementing detail coefficients to the already-computed approximation coefficients. If the second option is adopted, all the approximation coefficients at the next finer level of resolution have to be computed. The already-computed approximation coefficients at current level of resolution will be wasted. The computational cost is higher in this case.

The second generation wavelets should be utilized in the MRA of the updating stiffness information. The reason is explained as follows. The sampling points of the wavelet and scaling function in the FE model is determined by the position of the nodes of the elements, which are distributed unevenly in a bounded domain. This situation cannot be dealt with by the traditional wavelet, which works for even sampling in unbounded domain. The second generation wavelet, on the other hand, can be adapted to uneven sampling and finite boundaries, therefore, is utilized in this paper.

4. Lifting the lazy wavelet to the interpolating second generation wavelet

Lifting scheme was proposed by Sweldens (1996, 1997) to form more complex wavelets from simpler ones. One application of the methodology is to build the bi-orthogonal second generation wavelet of interpolating type from the Lazy wavelet. The process involves two steps: dual lifting and lifting.

The Lazy wavelet is nothing but sub-sampling operators applied on a discretized function/signal to separate even indexed and odd indexed samples. The operator for even sub-sampling is defined as E and the operator for odd sub-sampling is defined as D . The multi-resolution analysis operator from space V_{j+1} to its subspace V_j is define as \tilde{H} , and the operator from V_{j+1} to W_j as \tilde{G} , the corresponding inverse operator are H and G , respectively.

The filter operators of a Lazy wavelet can be presented as

$$H_j^{Lazy} = \tilde{H}_j^{Lazy} = E \quad (11a)$$

$$G_j^{Lazy} = \tilde{G}_j^{Lazy} = D \quad (11b)$$

Define operator \tilde{S} as $\tilde{S}_j = H_j^{int} D^*$, where H_j^{int} is an interpolating filter. By using the dual lifting scheme, which corresponds to the prediction step in the work of Sweldens (1996, 1997), a set of bi-orthogonal filters may be obtained as

$$H_j^{int} = E + \tilde{S}_j D \quad (12a)$$

$$\tilde{H}_j^{int} = E \quad (12b)$$

$$G_j^{int} = D \quad (12c)$$

$$\tilde{G}_j^{int} = D - \tilde{S}_j^* E \quad (12d)$$

With the following lifting scheme, which corresponds to the updating step, one has

$$H_j = H_j^{int} = E + \tilde{S}_j D \quad (13a)$$

$$\tilde{H}_j = \tilde{H}_j^{int} + S_j \tilde{G}_j^{int} = (1 - S_j \tilde{S}_j^*) E + S_j D \quad (13b)$$

$$G_j = G_j^{int} - S_j^* H_j^{int} = -S_j^* E + (1 - S_j^* \tilde{S}_j^*) D \quad (13c)$$

$$\tilde{G}_j = \tilde{G}_j^{int} = D - \tilde{S}_j^* E \quad (13d)$$

From these filters, the wavelet and scaling functions can be built. This scheme allows the adaptation of the wavelet to irregular supports and finite boundaries. By using interpolating operator of different number of interpolating points, various types of scaling and wavelet functions may be formed. This is usually achieved by so called ‘‘Cascade algorithm’’ (Sweldens and Schroder 1996). As the second generation wavelet is adapted to uneven sampling and finite

boundaries, the scaling functions and wavelet functions are also adapted to particular approximation level and sampling position.

5. The two-step updating strategy

The damage identification is usually performed with simplified models because they appear to be more cost effective and stable. The structure shown in Figs. 2 and 3, for instance, may be modeled by tapered beam elements, and the updating process may be carried out by utilizing the beam model. Because the beam model may not be able to duplicate the behavior of the undamaged real structure precisely, initial modeling error may be introduced in the simplified beam model. In this case, the mode shapes and frequencies of the simplified beam model may not match those of the real structure perfectly. Moreover, the mechanical behavior of the structure may become even more complex near the position of damage, which may not be possible to be represented simply by a beam model, hence updating error will also appear at the updating stage for damage identification.

This problem cannot be solved by involving more modal modes. Because the behavior of higher order mode of the real structure may deviate from the characteristic of an ideal beam even more notably, the introduction of the higher order modal information may do more harm than good to the identification.

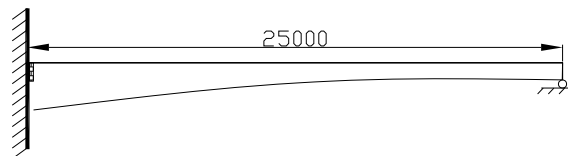


Fig. 2 Sketch of the beam (damage indicated by the circle) dimension in mm

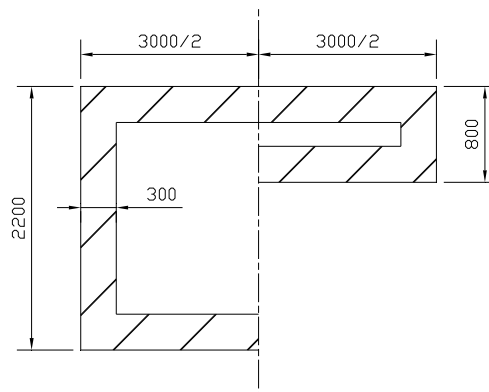


Fig. 3 Cross-section of the Beam, Dimension in mm

Therefore, we propose a two stage updating strategy:

a). Calibrating the simplified model against a more precise FE model or the undamaged real structure by minimizing the norm of the vector in Eq. (10). The error index is computed with modal parameters of simplified model and the more precise FE model or undamaged structure. In this step we obtain a calibration curve of stiffness.

At this stage, we degenerate the geometrically complex real structure to a geometrically simple structure to ease the numerical burden of the updating. If the model to be updated is three-dimensional, as in the example, the updating information is also three-dimensional and need multi-dimensional wavelet to represent, which is more complex to handle. For a beam element model, one dimensional wavelet is applicable.

The meshing of the simplified model may be as fine as desired. Although the resolution of the calibration curve of stiffness is impaired by the limited modal information available, the scaling functions and the wavelet functions may perform as interpolation operators to translate the limited number of updating coefficients into the element information within the model boundary.

The nature of the calibration procedure is to superimpose a lower resolution calibration stiffness function, $\kappa_A(x)$, onto a higher resolution pre-defined stiffness function $K(x)$ as stated in Eq. (1).

b). Updating the calibrated simplified model against the modal information of the damaged structure to find another updating curve of the stiffness reduction, $\kappa_B(x)$. The computation method is the same as step a). This curve is to be superimposed onto the resultant stiffness function obtained in step a). In this step, the damages are identified by observing the major features of the stiffness reduction curve. For the same reason mentioned above, the updating curve of the stiffness reduction is also low in resolution.

6. Numerical validation

The following example demonstrates the proposed updating method for damage identification. The material of the box girder shown in Figs. 2 and 3 is concrete, whose Young's modulus $E = 3 \times 10^{10} Pa$ and Poisson ratio $\gamma = 0.2$. The structure is modeled by a fine FE model with 7500 plate elements. A concentrated crack is simulated by releasing some nodes in the upper flange at the fixed end. A simplified FE model is also established by using 128 tapered beam elements, whose mechanical parameters are computed by using the geometrical and material properties of the box girder. The computation with ANSYS shows, in Table 1, the differences between the modal parameters of undamaged plate element and simplified beam models. Only vertical modes are shown in the table to simplify the discussion.

Table 1 Frequencies of the Vertical Modes

Frequency	f_1	f_2	f_3
Undamaged plate element model	7.487	21.274	39.734
Damaged plate element model	6.849	19.787	35.054
Undamaged beam model	6.257	18.865	38.530

The results in Table 1 indicate the initial modeling error exists for the beam element model and the calibration of simplified model is needed. In order to do so, we define the virtual work of the internal force of the beam model as

$$W_I = \int_0^l \delta \left[\frac{\partial^2 u}{\partial x^2} \right] K(\tilde{x}) \frac{\partial^2 u}{\partial x^2} dx \quad (14)$$

where u is the nodal displacements and $K(\tilde{x})$ is the stiffness matrix function to be represented in MRA format.

As in the common FE theory, after applying the principle of virtue work, the element stiffness function may be obtained as

$$K_{nm}^e = \int_0^l K(\tilde{x}) q_n''(x) q_m''(x) dx \quad (15)$$

Where $q_i(x)$ is the shape function for beam element corresponding to i^{th} degree of freedom and $q_i''(x) \equiv \frac{\partial^2 q_i}{\partial x^2}$. Substituting (1) and (5) into (15), we have

$$K_{nm}^e = \int_0^l [K(\tilde{x}) + \sum_k c_k^j \phi_{j,k}(\tilde{x}) + \sum_k d_k^j \psi_{n,k}(\tilde{x})] q_n''(x) q_m''(x) dx. \quad (16)$$

FE model at different approximation levels can be built by utilizing Eq. (16). Four points interpolation filter (Sweldens and Schroder 1996) is used for the second generation wavelet in this paper. Fig. 4 shows the computed scaling function and the wavelet function at the lowest resolution level, i.e. level 0. There are 5 sampling points for the scaling function and 4 sampling points for the wavelet function at level 0. The boundary effect is automatically taken into account in the lifting process as can be seen in the figure.

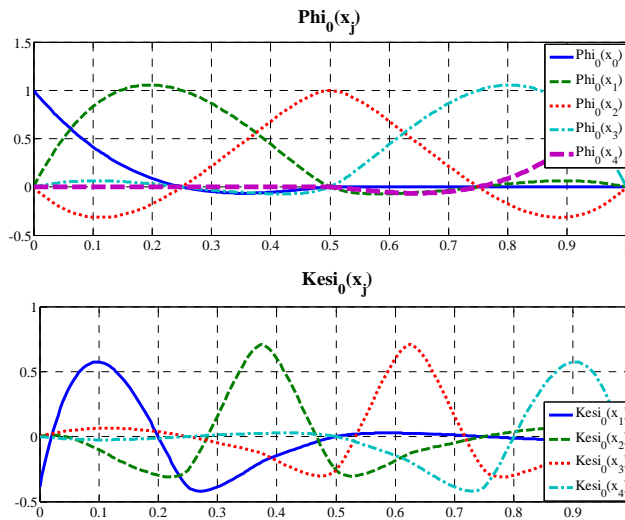


Fig. 4 The Scaling Function and Wavelet Function at Level 0

The FE model for the simplified model can be built using (16). After solving the eigen-equation of the simplified FE model, the error vector $\{r(\boldsymbol{\alpha})\}$ in (10) can be computed and its norm is minimized with GA to produce the approximation and wavelet coefficients.

The following updating is performed at approximation level 0 and 1 to check convergence of the method:

- At level 0, updating is performed by assigning $d_k^j = 0, j = 0$ to recover $c_k^j, j = 0$ only;
- On the basis of a), assume $d_k^j \neq 0, j = 0$ to find $d_k^j, j = 0$ and
- At level 1, updating is performed by assigning $c_k^j, d_k^j \neq 0, j = 0$ to find $c_k^j, d_k^j, j = 0$ together.

The results are shown in Figs. 5-7 as updating stage A. Fig. 5 shows the updating coefficients obtained in step b). The approximation (scaling) coefficients are indexed in the figure as 1,2,3,4,5 and detail (wavelet) coefficient as 6,7,8,9. These data represent the amplitudes of the scaling and wavelet functions. Fig. 6 shows the resultant stiffness. In the figure, “Initial” stands for the pre-defined stiffness of the beam elements computed via the geometrical dimensions of the box girder; “L0” represents the identified stiffness in step a); “L0+D0” is the result from step b) and “L1” the result of step c). It can be observed that the solutions at level 0 and 1 are close, indicating that the computation is converging.

The residues in the error vector are shown in Fig. 7. In the figure, “L0” and “L1” represent level 0 and level 1 approximations, respectively; indices 1-3 indicate the relative error of first three natural frequencies in percentage and indices 4-6 stands for the $1 - MAC$ values of the first three mode shapes. It can be seen that the residues are satisfactorily small.

After the calibration, the beam model is updated against the damaged model. The results are shown in Figs. 5 and 8 as updating stage B and as “DID-L1” in Fig. 6. The corresponding stiffness reduction curve is shown in Fig. 9.

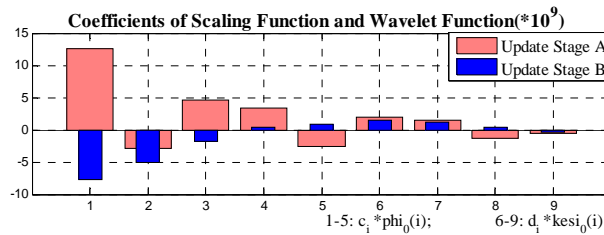


Fig. 5 Updating Coefficients of Scaling and Wavelet Functions

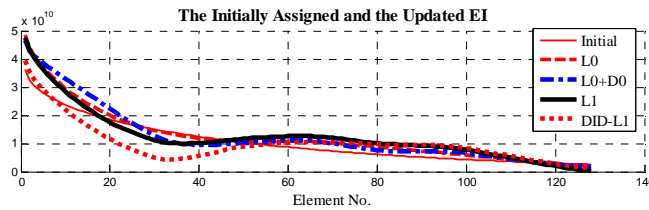


Fig. 6 Updated EI

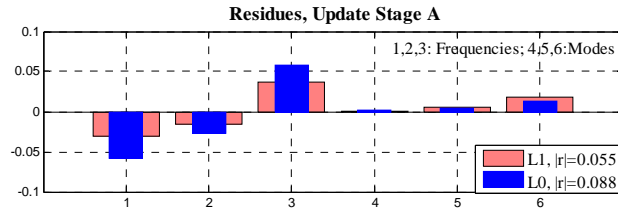


Fig. 7 Residues of the Error Vector in Update Stage A

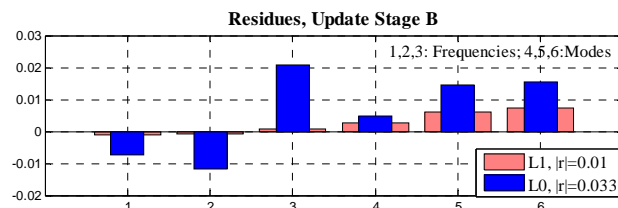


Fig. 8 Residues of the Error Vector in Update Stage B

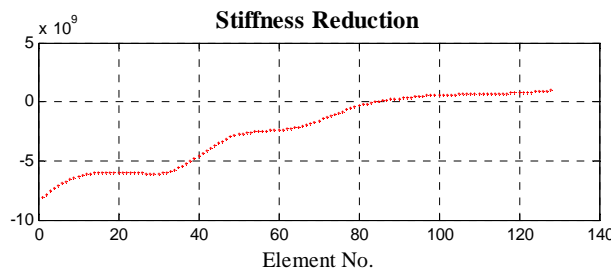


Fig. 9 Curve of the Stiffness Reduction

It can be judged from Fig. 9 that the concentrated crack at the fixed end causes a decrement of the stiffness in a number of beam elements. The position of the crack is indicated by the lowest portion of the curve. As the proposed method intends to identify the low resolution version of the stiffness reduction curve, it is reasonable that the main feature of the damage spread out across the affected region. It is like using a low pass filter to process a sharp “spike” signal, which will remove the sharp component and give rise to a spread out, less concentrated, moderately sloped curve.

7. The stability of the proposed method

It has been stated in section 2 that the MRA based model updating method is to find the “approximated curve” instead of the “real stiffness curve” in Fig. 1. Therefore, it is important that the “approximated curve” reflect the global feature of the real curve and is not very sensitive to

small changes in the configuration of structural damages. For example, as shown in figure 1c, the shape of the “approximated curve” should not change significantly when the number of the irregular cracks changes or when the intensity of these cracks varies. Because such variations in the configuration of damage also bring about perturbations in modal parameters, which are the corner stone of model updating, the stability of the proposed method against the perturbations of modal parameters due to small variations of the damage configuration has to be checked.

Three damage cases (Fig. 10) of the beam in Figs. 2 and 3 are designed to perform the stability check. In case 1, the beam has a crack, Cr_1 , at the fixed end; In case 2, the beam has three parallel cracks, $Cr_1+Cr_2+Cr_3$, at the fixed end; in case 3, in addition to the three cracks in case 2, the beam also has another three cracks, indicated as Cr_4 in the figure, at the region of positive moment. All adjacent cracks are separated by 1m.

The definition of damage cases and the corresponding modal parameters are summarized in Table 2. The identified stiffness reduction curves are shown in Fig. 11.

The following observations are made from Fig. 11:

a) It is noted that the depth of the crack in case 1 is shallower than the case in Fig. 9, therefore, the value of stiffness reduction is also smaller than Fig. 9, but the shapes of the curves in these two cases are similar, indicating the updating results are stable to the changes of the crack depth.

b) Case 2 has more cracks than case 1, therefore, has a larger reduction of stiffness. The shapes of the stiffness reduction curve are similar in cases 1 and 2, indicating the updating results are stable to the changes of the number of adjacent cracks.

c) Case 3 has the same damage condition as case 2 on the left hand side of the beam; therefore, the curves in case 2 and 3 are almost identical at this part. This also shows the numerical stability of the proposed method.

d) Compared to case 2, case 3 has three more cracks at the positive moment region. The stiffness reduction curve in case 3 has a dip at the position of cracks (around element no. 80). The method is effective to identify multiple groups of cracks.

The case study above shows that the proposed MRA-based model updating method corresponds to the global feature of the structural damage and is stable against the small changes of the damage.

Table 2 Combination of Cracks for Stability Study

Case	Combination of Cracks				Frequency (Hz)		
	Cr1	Cr2	Cr3	Cr4	f_1	f_2	f_3
1	Y				6.38	18.91	38.55
2	Y	Y	Y		5.79	18.47	36.70
3	Y	Y	Y	Y	4.67	17.41	34.13

Note: 1. The cracks are simulated by assigning the damaged element with a small Young's Modular.

2. Cr4 is a crack group of three parallel cracks separated by 1m.

3. The frequencies listed are the first three vertical mode frequencies.

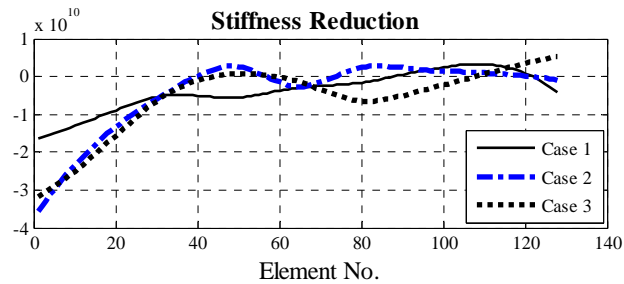


Fig. 11 Stability of the MRA-Based Model Updating

8. Refining the identification results

As explained in section 5 and further confirmed in section 6, the identified stiffness reduction curves suffer from the issue of information spreading-out due to the fact that we are working on low levels of resolution.

This issue can be partly circumvented given some fundamental understandings of the relationship between the true stiffness reduction curve and its low resolution representation. Based on the experiences from numerical experiments, we have the following statements:

- 1) The true stiffness reduction curve due to a concentrated crack is a spike. The low resolution representation of the spike is a “valley curve” whose minima locate at the position of the spike.
- 2) The true stiffness reduction curve due to a group of closely spaced multiple cracks is a series of spikes. The corresponding low resolution representation is a “basin curve” possibly with a flat bottom. If the resolution is too low, the “basin curve” becomes a “valley curve”.
- 3) Because the wavelet is a decaying wave, the superposition of the wavelet and scaling function gives rise to a fluctuating curve. The fluctuating curve may decay slowly at positions away from the spike.
- 4) The decaying feature applies both to the “valley curve” and “basin curve”.
- 5) The fluctuations of the low resolution curve may create “shadows” making the neighboring small damages difficult to identify.

Based on these understandings, a method to refine the identification in section 5 and 6 may be provided. The procedure is as follows:

- 1) Compute the low resolution stiffness reduction curve in the same way as in section 5 and 6.
- 2) Identify the major feature, i.e., the major valleys/basins, of the low resolution curve.
- 3) Proceed to the next finer resolution level and set the values of the coefficients outside the major valleys/basins to zero. In this case, the updating algorithm produces a stiffness reduction curve of higher resolution, whose values outside the major valleys/basins are basically zero. This step is to limit the number of the coefficients to be retrieved by the updating process. If the damage pattern of the structure is not too complex, the next finer level of resolution may need no more non-zero coefficients than the current level.
- 4) Compute for the error vector in Eq. (7).
- 5) If the norm of the error vector becomes smaller, proceed to still next finer level of

- resolution in the same way as in step 3).
- 6) If the norm of the error vector increase, it is assumed that there may be smaller damages in the “shadows” of major valleys/basins. In this case, we may select the valleys/basins of the secondary importance and group them with major valleys/basins. Repeat the procedure from the step 3). The valleys/basins of the secondary importance are those valleys/basins whose fluctuations are larger than other valleys/basins but smaller than the major valleys/basins.
 - 7) The procedure continues until the result is acceptable.

This refinement procedure is applied to the stiffness reduction curves in Fig. 11. The results are shown in Fig. 12. It can be seen, the quality of the identification has been improved significantly.

9. The experimental validation

A concrete bridge is used to validate the proposed method. The bridge is a part of the City Express. Two parallel bridges carry the east-west traffic and west-east traffic respectively. The two parallel bridges were designed identical only with opposite crown slopes. The two bridges were constructed under the same contract. Due to overloading, the bridge carrying the west-east traffic cracked at the east span after 10 years in service. The position of the crack is known, but the value of stiffness reduction is not known. This creates a manageable condition for the application of the proposed method: the undamaged east-west bridge can be used as the reference bridge for the damaged west-east bridge to calibrate the FE model.

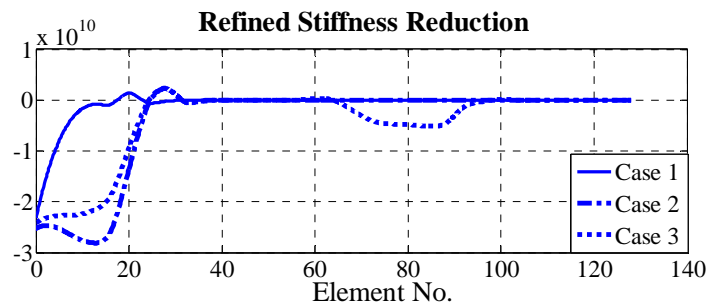


Fig. 12 Refined Stiffness Reduction Curve

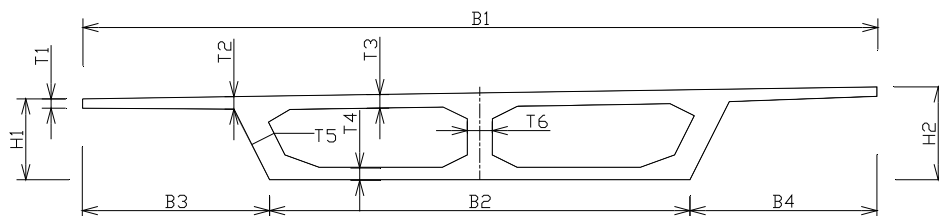


Fig. 13 Cross Section of the Experimental Bridge

The bridge is a three-span (25 m + 35 m + 25 m) simply supported continuous pre-stressed concrete box girder. The drawings of the bridge girder are shown in Figs. 13 and 14. The parameters in the Fig. 13 are not constant values along the span and listed in Table 3.

Operational modal testing was carried out on both of the two bridges. First three vertical modes were identified. The identified modal frequencies are listed in Table 4. A FE model of 128 tapered beam elements was built with MatLab for model updating. In order to accommodate the dyadic wavelet refinement process, each span should consist of 2^n elements. Therefore, the span where the damage exists is meshed with 64 elements; the other two spans are meshed with 32 elements.

At the calibration stage, the FE model was calibrated against the undamaged east-west bridge at level 1 by assigning $c_k^j, d_k^j \neq 0, j = 0$ for all the 128 elements. Because the cross section of the girder is almost constant, the modeling error of stiffness is not significant. The modal parameters of the calibrated FE model are listed in Table 4.

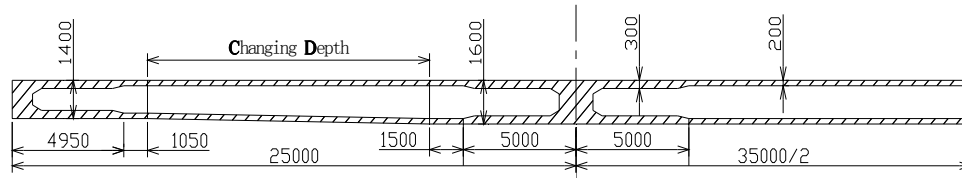


Fig. 14 Elevation of the Girder at the Central Line (dimension in mm)

Table 3 Parameters of the Bridge Cross Section

Parameters (m)		Parameters (m)	
B_1	12.75	T_1	0.150
B_2	6.75 or 6.55	T_2	0.450
B_3	3.1 or 3.0	T_3	0.2 or 0.3
B_4	6.75 or 6.55	T_4	0.2 or 0.3
H_1	1.504 to 1.304	T_5	0.4 or 0.5
H_2	1.620 to 1.496	T_6	0.5

Table 4 Vertical Modes Frequencies of the Bridge

Frequency	f_1	f_2	f_3
The undamaged east-west bridge	4.05	6.47	6.77
The damaged west-east bridge	3.90	6.20	6.65
The beam element model before calibration	4.00	6.4	6.71
The beam element model after calibration	4.04	6.48	6.77

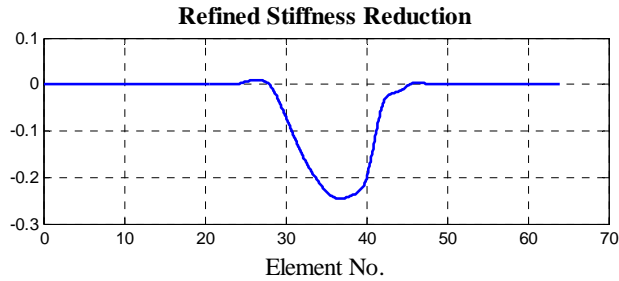


Fig. 15 Percentage of Stiffness Reduction-the Refined Result

At the damage identification stage, only the 64 elements in the damaged span are subjected to updating. The other 64 elements in the other two spans are kept the same as in the calibration stage. By the method stated in section 5 and the 7, the refined stiffness reduction curve is obtained and shown in Fig. 15. In the figure, the stiffness reduction is divided by the local stiffness of the undamaged beam. Therefore, the value in the figure is the percentage of stiffness reduction. The crack is known to exist at element no. 35. The identification result shows the damage is around element no. 36~37, and the stiffness reduction is about 25% of the original stiffness. The result correlates with the known information of damage well.

10. Conclusions

Based on the theory of multi-resolution analysis (MRA), the finite element (FE) model updating process is understood as the superposition of two pieces of information of different resolutions: the pre-defined stiffness information and the updating stiffness information. The resolution of the former is determined by the meshing density of the FE model, the resolution of the latter, on the other hand, is determined by what we can retrieve from the experiments. The latter is unavoidably lower than the former in resolution. With the help of the second generation wavelet, the updating stiffness can be represented in the form of MRA using fewer coefficients for the wavelet and scaling functions to picture the major features of the updating information. After the identification of the major features, the refinement process proposed in this paper can bring the updating to the next finer levels of resolution. The damage identification becomes clearer and more reliable.

The MRA of the updating stiffness information is not equivalent to the traditional wavelet decomposition of the corresponding data. It has to be performed in the context of the similarity of the eigen-systems. This is achieved in this paper by a two-stage method minimizing the error of the eign-parameters of the structural system followed by a refinement process.

The proposed method is validated by numerical simulations and experiments. The numerical simulations show that the method is stable to small changes of the crack depth and the number of adjacent cracks. It is effective to identify multiple groups of cracks. The experiments show the adaptability of the proposed method to the applications of real world situation.

References

- Bakir, P.G., Reynders, E. and Roeck, G.D. (2007), "Sensitivity-based finite element model updating using constrained optimization with a trust region algorithm", *J. Sound Vib.*, **305**(1-2), 211-225.
- Brownjohn, J.M.W., Xia, P.Q., Hao, H. and Xia, Y. (2001), "Civil structure condition assessment by FE model updating methodology and case studies", *Finite Elem. Anal. Des.*, **37**(10), 761-775.
- Esfandiari, A., Bakhtiari-Nejad, F., Sanayei, M. and Rahai, A. (2010), "Structural finite element model updating using transfer function data", *Comput. Struct.*, **88**(1-2), 54-64.
- Fang, S.E., Perer, R. and Roeck, G.D. (2008), "Damage identification of reinforced concrete frame by finite element model updating using damage parameterization", *J. Sound Vib.*, **313**(3-5), 544-559.
- Imregun, M., Visser, W.J. and Ewins, D.J. (1995), "Finite element model updating using frequency response function data—I. Theory and initial investigation", *Mech. Syst. Signal Pr.*, **9**(2), 187-202.
- Jaishi, B. and Ren, W.X. (2006), "Damage detection by finite element model updating using modal flexibility residual", *J. Sound Vib.*, **290**(1-2), 369-387.
- Mian, N.M.M. and Silva, J.M.M. (1997), *Theoretical and experimental modal analysis*, John Wiley & Sons INC.
- Jaishi, B. and Ren, W.X. (2007), "Finite element model updating based on eigenvalue and strain energy residuals using multi-objective optimization technique", *Mech. Syst. Signal Pr.*, **21**(5), 2295-2317.
- Kim, G.H. and Park, Y.S. (2008), "An automated parameter selection procedure for finite element model updating and its applications", *J. Sound Vib.*, **309**(3-5), 778-793.
- Kyprianou, A., Worden, K. and Panet, M. (2001), "Identification of hysteretic system using the differential evolution algorithm", *J. Sound Vib.*, **248**(2), 289-314.
- Law, S.S., Chan, T.H.T. and Wu, D. (2001), "Efficient numerical model for the damage detection of large scale", *Eng. Struct.*, **23**(5), 436-451.
- Levin, R.I. and Lieven, N.A.J. (1998), "Dynamic finite element model updating using simulated annealing and genetic algorithms", *Mech. Syst. Signal Pr.*, **21**(1), 91-120.
- Mallat, S. (2009), *A wavelet tour of signal processing: the sparse way*, (3rd Ed.), Elsevier Singapore.
- Mottershead, J.E., Link, M. and Friswell, M.I. (2011), "The sensitivity method in finite element model updating: A tutorial", *Mech. Syst. Signal Pr.*, **25**(7), 2275-22962.
- Perera, R. and Ruiz, A. (2008), "A multistage FE updating procedure for damage identification in large-scale structures based on multi-objective evolutionary optimization", *Mech. Syst. Signal Pr.*, **22**(4), 970-991.
- Ren, W.X. and Chen, H.B. (2010), "Finite element model updating in structural dynamics by using response surface method", *Eng. Struct.*, **32**(8), 2455-2465.
- Sweldens, W. (1996), "The lifting scheme: a custom-design construction of bi-orthogonal wavelets", *Appl. Comput. Harmon. A.*, **3**(2), 186-200.
- Sweldens, W. (1997), "The lifting scheme: a construction of second generation wavelets", *Siam J. Math. Anal.*, **29**(2), 511-546.
- Sweldens, W. and Schroder P. (1996), "Wavelets in computer graphics", SIGGRAPH 96 Course Notes.
- Teughels, A., Maeck, J. and Roeck, G.D. (2002), "Damage assessment by FE model updating using damage functions", *Comput. Struct.*, **80**(25), 1869-1879.
- Titurus, B., Friswell, M.I. and Starek, L. (2003), "Damage detection using generic elements: Part I. Model updating", *Comput. Struct.*, **81**(24-25), 2273-2286.
- Weng, S., Xia, Y., Xu, Y.L. and Zhu, H.P. (2011), "Substructure based approach to finite element model updating", *Comput. Struct.*, **89**(9-10), 772-782.
- Yu, E. and Chung L. (2012), "Seismic damage detection of a reinforced concrete structure by finite element model updating", *Smart Struct. Syst.*, **9**(3), 253-271.
- Yun, G.J., Ogorzalek, K.A., Dyke, S.J. and Song, W. (2009), "A two-stage damage detection approach based on subset selection and genetic algorithms", *Smart Struct. Syst.*, **5**(1), 1-21.
- Zapico-Valle, J.L., Alonso-Cambor, R., Gonzalez-Martinez, M.P. and Garcia-Dieguez, M. (2010), "A new

method for finite element model updating in structural dynamics”, *Mech. Syst. Signal Pr.*, **24**(7), 2137-2159.

CC

List of Symbols

α	State vector
c_j^k, d_j^k	Approximation and detail coefficients, respectively
D, E	Odd sub-sampling and even sub-sampling operator, respectively
$K(x)$	True stiffness of a structure
$K(x)$	The pre-defined stiffness function at position x
$\kappa(x)$	Updating function of stiffness
\tilde{H}, \tilde{G}	The operator from V_{j+1} to V_j and W_j , respectively
H, G	The operator from V_j and W_j to V_{j+1} , respectively
H_j^{int}	An interpolating filter
V_j, W_j	Functional Spaces
$\phi(x), \phi_{j,k}(x-k)$	Scaling function
$\psi(x), \psi_{j,k}(x-k)$	Wavelet function
$\tilde{\phi}_{j,k}(x)$	The dual of $\phi_{j,k}(x)$
$\tilde{\psi}_{j,k}(x)$	The dual of $\psi_{j,k}(x)$.
λ_i	The i^{th} frequency
φ_i	The i^{th} mode shape